

Changes in Murine Jejunal Morphology Evoked by the Bacterial Superantigen *Staphylococcus aureus* Enterotoxin B Are Mediated by CD4⁺ T Cells

MICHELLE A. BENJAMIN, JUN LU, GRAEME DONNELLY,
PARUL DUREJA, AND DEREK M. MCKAY*

*Intestinal Disease Research Programme, McMaster University,
Hamilton, Ontario, Canada L8N 3Z5*

Received 29 October 1997/Returned for modification 12 January 1998/Accepted 4 February 1998

Bacterial superantigens (SAGs) are potent T-cell stimuli that have been implicated in the pathophysiology of autoimmune and inflammatory disease. We used *Staphylococcus aureus* enterotoxin B (SEB) as a model SAG to assess the effects of SAG exposure on gut form and cellularity. BALB/c, SCID (lacking T cells) and T-cell-reconstituted SCID mice were treated with SEB (5 or 100 µg intraperitoneally), and segments of the mid-jejunum were removed 4, 12, or 48 h later and processed for histochemical or immunocytochemical analysis of gut morphology and major histocompatibility complex class II (MHC II) expression and the enumeration of CD3⁺ T cells and goblet cells. Control mice received saline only. SEB treatment of BALB/c mice caused a time- and dose-dependent enteropathy that was characterized by reduced villus height, increased crypt depth, and a significant increase in MHC II expression. An increase in the number of CD3⁺ T cells was observed 48 h after exposure to 100 µg of SEB. Enteric structural alterations were not apparent in SEB-treated SCID mice compared to saline-treated SCID mice. In contrast, SEB challenge of SCID mice reconstituted with a mixed lymphocyte population or purified murine CD4⁺ T cells resulted in enteric histopathological changes reminiscent of those observed in SEB-treated BALB/c mice. These findings implicate CD4⁺ T cells in this SEB-induced enteropathy. Our results show that SAG immune activation causes significant changes in jejunal villus-crypt architecture and cellularity that are likely to impact on normal physiological processes. We speculate that the elevated MHC II expression and increased number of T cells could allow for enhanced immune responsiveness to other SAGs or environmental antigens.

Evidence from clinical observations, animal models of disease, and studies with cell lines indicate an intimate association between bacteria (and bacterial products) and the pathophysiology of enteric inflammatory and secretory disorders (28, 30). Moreover, significant tissue damage and abnormal physiology can be attributed to aberrant immune reactions, where T cells have been identified as a key cell type (5). A novel group of bacterial products have been identified that cross-link major histocompatibility complex class II (MHC II) molecules with a variable portion of the β chain (Vβ) of the T-cell receptor, binding beyond the antigen-specific site. These molecules do not require classical antigen-processing and presentation and can polyclonally stimulate up to 25% of T cells based on Vβ specificity, hence their designation as superantigens (SAGs) (8, 14). Skewed expression of T-cell receptor Vβ usage has been used to implicate SAGs in the pathogenesis of autoimmune and inflammatory disorders such as rheumatoid arthritis and diabetes (7, 27). More recently it has been postulated that SAGs could be involved in the initiation or exaggeration of inflammatory bowel disease in some patients (13, 29).

Delineation of the physiological and pathophysiological effects, and mechanisms thereof, of exposure to SAGs has lagged behind the elucidation of the immunomodulatory properties of bacterial SAGs. The enterotoxins of the gram-positive *Staphylococcus aureus* are prototypic SAGs, and *S. aureus* enterotoxin

B (SEB) has been used extensively as a model SAG to define the effects of these bacterial products on immune cells (14). Many elegant studies have shown that the murine immune response to SAGs is biphasic: an initial activation phase characterized by T-cell proliferation, cytokine production, and enhanced cytotoxic activity (10, 17, 25) is followed by a period of anergy and/or depletion of the appropriate Vβ-expressing T cells (32, 34). In beginning to define the enteric physiological consequences of exposure to bacterial SAGs, the objective of the present study was to assess the impact of SEB treatment on jejunal structure and cellularity in immunocompetent (BALB/c) and T-cell-deficient (severe combined immunodeficient [SCID]) mice. Our data demonstrate that SEB treatment of normal but not T-cell-deficient mice evokes a self-limiting enteropathy that is characterized by altered villus-crypt architecture, various degrees of histopathology, increased MHC II expression, and an increase in CD3⁺ T cells. We suggest that these changes will disrupt normal enteric physiological and homeostatic processes and have the potential to predispose the host to enhanced immune responsiveness to other antigens that gain access to the mucosa and/or submucosa.

MATERIALS AND METHODS

Animals and experimental treatment. Male BALB/c mice (7 to 9 weeks old; Charles River Animal Suppliers, St. Constant, Canada) were housed in conventional facilities with free access to food and water and received a single intraperitoneal (i.p.) injection of 5 or 100 µg of SEB (Sigma Chemical Co., St. Louis, Mo.). Administration of SEB by this route was favored over oral treatment since many studies assessing the immunomodulatory effects of SEB have administered the SAG by i.p. injection. The amounts of SEB used here are representative of the low and high doses of SEB employed by other investigators examining the immunomodulatory properties of SAGs (10, 25). (Gram-positive bacteria do not produce lipopolysaccharide and the stocks used in these experiments were not

* Corresponding author. Mailing address: Intestinal Disease Research Programme, HSC-3N5, Department of Pathology, McMaster University, 1200 Main St. W., Hamilton, Ontario, Canada L8N 3Z5. Phone: (905) 525-9140, ext. 22588. Fax: (905) 522-3454. E-mail: mckayd@fhs.McMaster.ca.

TABLE 1. Murine serum IL-2 levels

Mouse strain or type ^a	Serum IL-2 level (ng/ml) with SEB treatment regimen (time of dose, amt) ^b				
	0	4 h, 5 μ g	4 h, 100 μ g	48 h, 5 μ g	48 h, 100 μ g
BALB/c	13.7 \pm 1.3	43.5 \pm 14.7*	60.2 \pm 11.4*	18.6 \pm 16.4	48.9 \pm 13.3*
SCID	0	0	NT ^c	NT	NT
recon-SCID	NT	72.9 \pm 28.7*	NT	NT	NT
CD4 ⁺ T-cell-SCID	3.5 \pm 2.1	137.3 \pm 36.4*	NT	NT	NT

^a recon-SCID, SCID mice reconstituted with a mixed BALB/c spleen and mesenteric lymph node cell population; CD4⁺ T-cell-SCID, SCID mice reconstituted with BALB/c CD4⁺ T cells.

^b Mice were administered SEB i.p. in the indicated amounts at the indicated times before sacrifice. Values are means \pm SEM; $n = 3$ to 5. *, $P < 0.05$ compared to nontreated BALB/c or SCID mice.

^c NT, not tested.

contaminated with lipopolysaccharide as determined by the *Limulus* amoebocyte assay [Sigma Chemical Co.]. Mice were sacrificed by cervical dislocation at 4, 12, or 48 h after SEB treatment; these time points were based on our data showing changes in jejunal electrolyte transport following SEB treatment (20). Control mice received phosphate-buffered saline (PBS) only (vehicle for SEB administration). At sacrifice, the abdominal cavity was opened and pieces of jejunum were excised 12 cm distal to the ligament of Treitz.

In other experiments, the effect of SEB on jejunal morphology in SCID/beige mice was assessed. In these animals functional mature T and B cells are absent or drastically reduced in number (2). SCID mice were bred in the animal care facility at McMaster University and following weaning were housed in autoclaved microisolator cages. The mice were given sterile food and were maintained on an alternating regimen of normal water and water containing the antibiotics trimethoprim-sulfamethoxazole. Additional SCID mice were reconstituted with a

mixed lymphocyte population or purified CD4⁺ T cells from BALB/c mice, and the effects of i.p. administration of SEB were examined. Briefly, spleens and mesenteric lymph nodes from normal BALB/c mice were excised and mechanically dispersed into a single-cell suspension, and the erythrocytes were lysed by a 2-min incubation in ammonium chloride buffer. After centrifugation, the immune cells were resuspended in sterile PBS, and 30×10^6 cells in 0.2 ml of PBS were injected into the tail veins of SCID mice. Alternatively, after erythrocyte lysis, the mixed immune cell population was resuspended in RPMI culture medium (containing 10% fetal calf serum and antibiotics; Gibco BRL, Burlington, Canada) and incubated for 2 h at 37°C on sterile petri dishes to remove adherent macrophages. CD4⁺ T cells were then positively selected from the nonadherent lymphocyte population by MACs magnetic cell sorting (Miltenyi Biotec Inc., Auburn, Calif.). Lymphocytes (10^7) were incubated with 10 μ l of colloidal super-paramagnetic microbeads conjugated to rat anti-mouse CD4

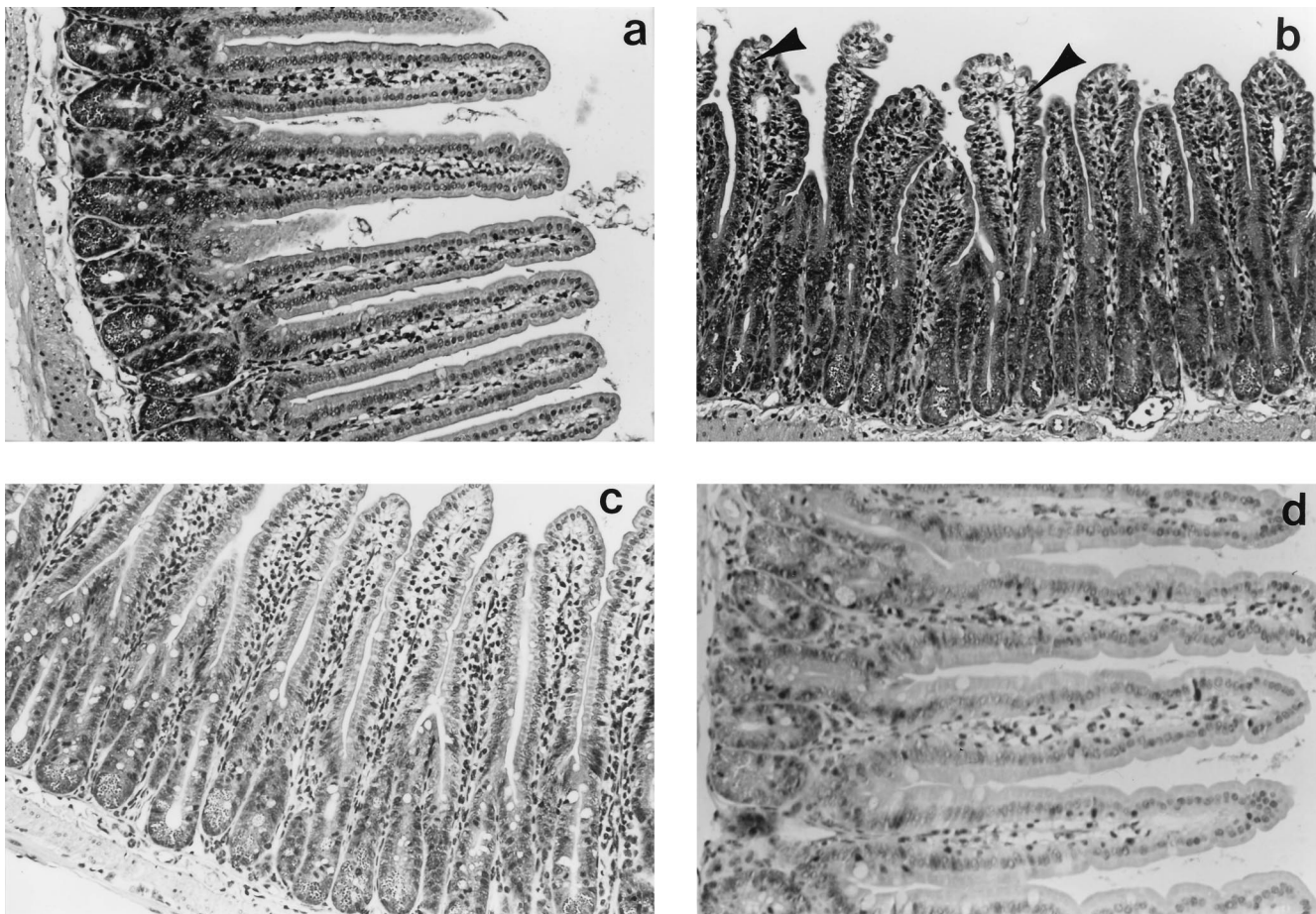


FIG. 1. Photomicrographs of jejunal morphology in a control BALB/c mouse (a) and in experimental mice 4 (b), 12 (c), and 48 (d) h after challenge with 5 μ g of SEB. After SEB treatment, villi are stunted and swollen, with evidence of edema, hypertrophy, and epithelial vacuolation (panel b, arrowheads). Also note crypt elongation 4 and 12 h after SEB treatment. Magnification, $\times 1,200$ (a to c) or $\times 1,500$ (d).

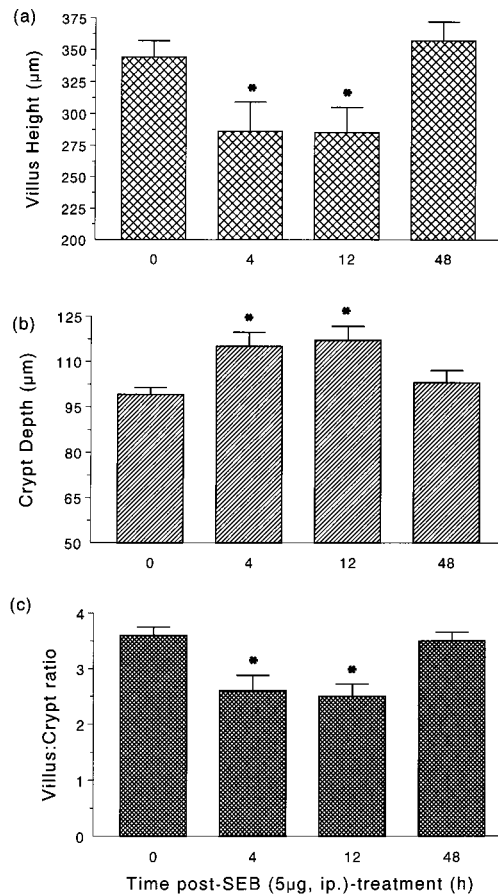


FIG. 2. Bar charts showing changes in villus height (a), crypt depth (b), and the villus:crypt ratio (c) in the jejunum of BALB/c mice treated with SEB ($n = 10$). *, $P < 0.05$ compared to control mice.

antibodies (L3T4; Miltenyi Biotec Inc.) for 20 min at 4°C , and the cell suspension was passed through an LS⁺ column mounted in a Midi-MACs magnet. After being washed with buffer (PBS, 2 mM EDTA, 0.5% [wt/vol] bovine serum albumin), the column was removed from the magnet and the CD4⁺ T cells were eluted with cold buffer. The positively selected CD4⁺ cells were resuspended in sterile PBS, and 15×10^6 cells in 0.2 ml of PBS were administered via the tail vein to SCID mice. Four to six weeks later the reconstituted SCID mice were treated with SEB.

These experiments were conducted under the guidelines of the McMaster University Animal Care Committee.

Immune activation. (i) IL-2. Blood samples were collected and serum was stored at -70°C prior to measurement of interleukin 2 (IL-2) levels as an indication of specific T-cell activation. IL-2 determinations were conducted by the sandwich enzyme-linked immunosorbent assay technique and with paired capture and detection antibodies from PharMingen Inc. (Mississauga, Canada). All determinations were performed in duplicate and in 3 serial dilutions.

(ii) MHC II antigen expression. Segments of intestine were snap frozen in liquid N₂ in O.C.T. compound (Sakua Finetek USA Inc., Torrance, Calif.), and 8- μm thick cryosections were cut, collected on 9-aminoalkylsilane-coated slides, and immediately postfixed for 15 min at room temperature (RT) in acetone. Following three PBS washes, sections were incubated in 1% bovine serum albumin for 15 min and then incubated for 60 min in a 1:200 dilution of a rat anti-mouse monoclonal anti-MHC II biotinylated antibody (IAc; provided by D. P. Snider, McMaster University). Sections were washed and incubated in a streptavidin-peroxidase solution for 20 min at RT. Color development was achieved by treatment with aminoethylcarbazole chromogen-substrate (0.05 M acetate buffer [pH 5.0], 0.003% [wt/vol] aminoethylcarbazole [stock diluted in dimethylformamide], 0.003% H₂O₂; all from Sigma Chemical Co.) for 15 min at RT. The sections were then counterstained with Mayers hematoxylin and viewed and photographed by a single investigator.

Histological assessment. Portions of small intestine were opened along the mesenteric border and immersion flat fixed in 10% neutral-buffered formalin. After fixation, tissues were dehydrated through graded alcohols and embedded

in paraffin wax, and 3- μm sections were cut perpendicular to the long axis of the villi.

(i) Villus-crypt and mucosal morphology. Histological sections on coded slides were stained with hematoxylin and eosin and examined by two investigators and a histopathologist for evidence of immune cell infiltrate and intestinal damage. Complete villus-crypt units were defined on the basis of a uniform intact epithelial lining and a rounded villus tip (22). Villus height and crypt depth were determined for 6 to 10 villus-crypt units per mouse with a $\times 20$ objective and a calibrated eyepiece graticule, and the villus:crypt ratios were calculated.

(ii) Goblet cells. Additional tissue sections were stained with the periodic acid-Schiff reagent (PAS) technique for mucopolysaccharides. Mucus-containing goblet cells were counted, and numbers are expressed per micrometer of basement membrane (villus height plus crypt depth).

(iii) CD3⁺ T cells. T cells were identified by indirect immunocytochemistry. After rehydration the tissue sections were incubated in a 0.05% (vol/wt) solution of trypsin in Tris buffer containing 0.25% CaCl₂ for 30 min at 37°C . After being rinsed, the sections were incubated in normal goat serum for 15 min at RT and then exposed to rabbit anti-human polyclonal anti-CD3 antibodies (1:200 dilution in normal goat serum [no. 3A0452; Dako Diagnostics Inc., Mississauga, Ontario, Canada]) for 60 min at RT. (The antibodies used cross-react with mouse CD3.) Sections were rinsed in Tris buffer, incubated for 30 min at RT in biotinylated swine anti-rabbit antibodies (1:300 dilution [no. E353; Dako Inc.]), rinsed again, incubated in a streptavidin-peroxidase solution for 10 min at RT and developed as above. After being counterstained with hematoxylin, the sections were mounted in glycerin gelatin and viewed. Total CD3⁺ cells and CD3⁺ cells in the epithelial villar compartment were counted, and data are expressed per 100 μm of villus basement membrane.

Analysis. All data are expressed as means \pm standard errors of the means (SEM). The n value represents the number of animals in each group. Multiple group comparisons were made by using a one-way analysis of variance followed by post-hoc intergroup comparison with the Newman-Keuls test. Where appropriate, Student's t test was used to compare two groups. A level of statistically significant difference was accepted at $P < 0.05$.

RESULTS

Immune activation. (i) IL-2. Serum levels of IL-2 were significantly elevated in BALB/c mice in response to a single low (5 μg) or high (100 μg) dose of SEB (Table 1). In contrast IL-2 was not detected in serum from the immunocompromised SCID mice or SCID mice challenged 4 h previously with SEB. However, SCID mice reconstituted with lymphocytes or CD4⁺ T cells from normal BALB/c mice did show increased IL-2 production following exposure to SEB.

(ii) MHC II antigen expression. Immunocytochemical staining for MHC II revealed diffuse staining in the lamina propria and mucosa of jejunal segments from control mice. This distribution pattern is consistent with a network of dendritic cells and macrophages in the gut. Under the conditions used only faint or negligible MHC II expression was detected in the epithelium. Assessment of jejunal sections from mice treated 4 or 48 h previously with 5 μg of SEB revealed a pattern of MHC II expression that was not appreciably different from that in control tissues. However, mice treated 48 h previously with 100 μg of SEB showed more abundant MHC II expression throughout the lamina propria (staining was more intense) and patchy expression in the epithelium (data not shown).

Histological assessment. Histological sections from time-matched control (PBS-treated) mice had normal jejunal morphology, with elongate villi, a complete epithelial lining, and no

TABLE 2. Jejunal villus-crypt structure in SEB-treated BALB/c mice^a

SEB treatment regimen	Villus length (μm)	Crypt depth (μm)	Villus:crypt ratio
Control	368 \pm 35	100 \pm 2	3.7 \pm 0.3
4 h, 100 μg	286 \pm 15**	125 \pm 9*	2.3 \pm 0.1*
48 h, 100 μg	298 \pm 7**	153 \pm 7*	2.0 \pm 0.2*

^a SEB was administered i.p. at 4 or 48 h prior to sacrifice. Values are means \pm SEM; $n = 4$ for all groups. *, $P < 0.001$ compared to control; **, $P = 0.05$ compared to control.

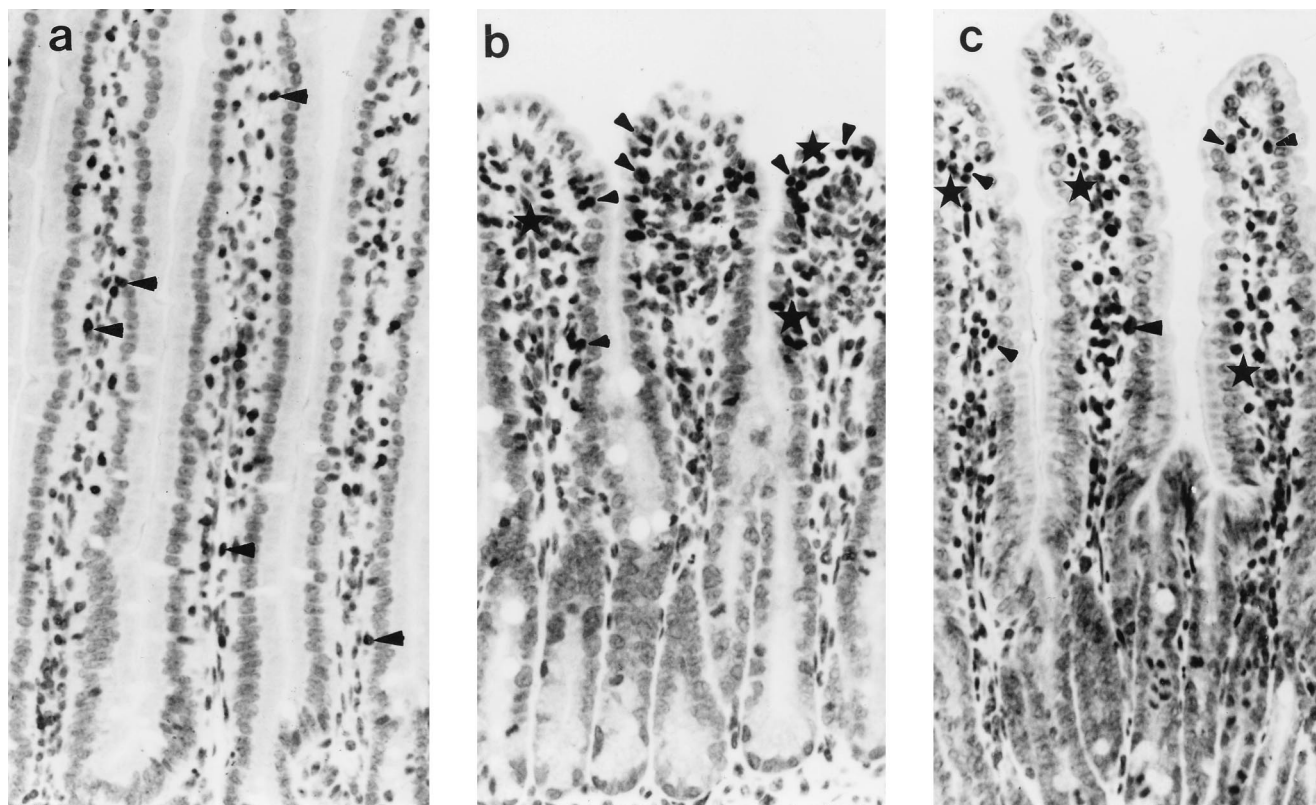


FIG. 3. Photomicrographs showing immunostaining of CD3⁺ T cells in the jejunum of a control BALB/c mouse (a) and mice treated with 5 µg of SEB 4 (b) and 48 (c) h previously. Note in panel b the altered villus-crypt morphology and the concentration of cells at the villus tip (some CD3⁺ cells are denoted by arrowheads and the asterisks indicate clusters of four or more CD3⁺ T cells). Magnification, ×160.

overt signs of major edema, tissue damage, or inflammatory infiltrate (Fig. 1). Jejunal sections from SEB (5 µg)-treated mice showed various degrees of edema, swelling of the villus lacteal, and increased epithelial vacuolation around the nucleus and at the apical pole of the cell; vacuolation was particularly obvious in cells at the villus tip (Fig. 1). However, a complete epithelial layer was consistently observed. An obvious neutrophilic or eosinophilic infiltrate was not observed, although neutrophils were often observed in the vasculature at the base of the crypts. Paneth cell granules were prominent in tissue from treated animals. These changes in gut structure were apparent 4 and 12 h after SEB treatment, while tissue from mice treated 48 h previously with 5 µg of SEB appeared histologically normal. Similar changes were observed in jejunal sections from mice treated with 100 µg of SEB.

(i) **Villus-crypt morphology.** Morphometric analysis revealed a significant reduction in villus height and an increase in crypt depth at 4 and 12 h post-SEB (5 µg) treatment (Fig. 1 and 2); however, villus erosion was not apparent. These changes in villus-crypt morphology resulted in an ~30% decrease in the villus: crypt ratio (Fig. 2c), which returned to control levels by 48 h posttreatment. These alterations in villus-crypt architecture were prolonged by administration of the high (100 µg) dose of SEB (Table 2), being still apparent 48 h after treatment.

(ii) **Goblet cells.** Enumeration of PAS-positive, mucus-containing goblet cells revealed a small reduction in the number of such cells in tissue from mice treated 48 h previously with SEB (5 µg) compared to that in tissue from controls (1.9 ± 0.4 versus 2.8 ± 0.2 goblet cells/100 µm of basement membrane [$n = 5$, $P = 0.05$]). Exposure to SEB for 4 or 12 h did not result

in a significant change in the number of PAS-positive goblet cells compared to that in the control mice.

(iii) **CD3⁺ T cells.** Immunocytochemical staining of T cells showed that in tissue from SEB-treated animals there was a qualitative increase in the distribution of CD3⁺ cells and greater numbers of cells in the intraepithelial compartment or juxtaposed to the epithelial basement membrane (Fig. 3). CD3⁺ cell counts are given in Table 3. There was a trend towards an increase in total CD3⁺ cells, and intraepithelial CD3⁺ T cells, in the intestines of SEB (5 µg)-treated mice which, due to intermouse variability, did not reach statistical significance. However, there was a twofold increase in total CD3⁺ T cells and intraepithelial CD3⁺ T cells in the jejunum of mice treated 48 h previously with SEB (100 µg).

TABLE 3. Immunocytochemical enumeration of CD3⁺ T cells in the jejunum of BALB/c mice after SEB treatment

SEB treatment regimen ^a	<i>n</i>	CD3 ⁺ cells ^b	CD3 ⁺ intraepithelial T cells ^b
Control	7	4.1 ± 0.6	2.6 ± 0.4
4 h, 5 µg	6	6.6 ± 2.5	4.1 ± 1.6
12 h, 5 µg	6	7.7 ± 1.8	4.4 ± 1.1
48 h, 5 µg	6	3.9 ± 0.9	2.3 ± 0.6
4 h, 100 µg	4	6.6 ± 1.4	3.6 ± 0.7
48 h, 100 µg	4	8.7 ± 0.8*	5.2 ± 0.4*

^a SEB was administered i.p. in the indicated amounts and at the indicated times prior to sacrifice.

^b Cell counts are expressed as numbers of cells/100 µm of basement membrane. Values are means ± SEM. *, $P < 0.05$ compared to control.

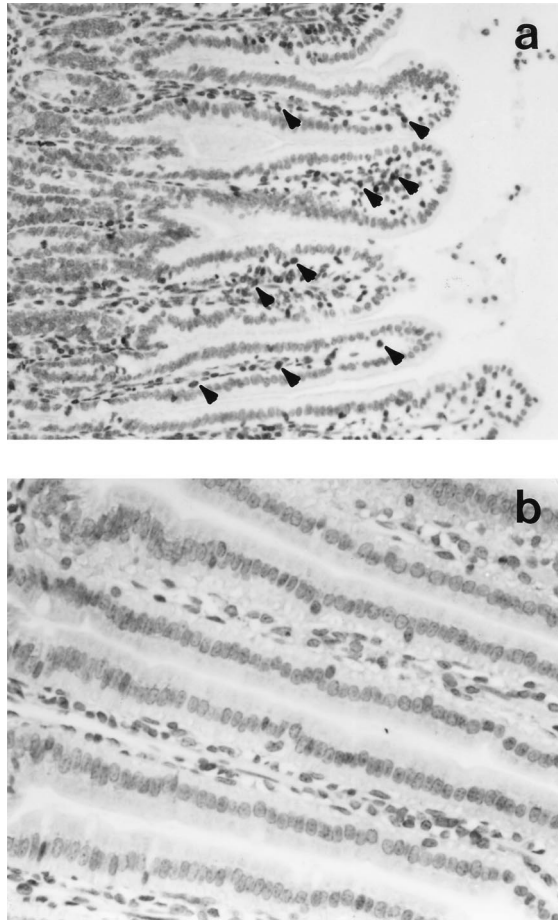


FIG. 4. Photomicrographs showing immunostaining of CD3⁺ T cells in the jejunum of a T-cell-reconstituted SCID mouse (a) and of a normal SCID mouse (b) 4 h after SEB challenge. T cells are readily apparent (arrowheads) in the lamina propria and mucosa of the reconstituted SCID mouse but were not identified, even at a higher magnification, in the jejunum from normal SCID mice. Magnification, $\times 200$ (a) or $\times 250$ (b).

SCID mice and T-cell-reconstituted SCID mice. Figure 4a shows CD3⁺ T cells in the intestine of a T-cell-reconstituted mouse, whereas normal SCID mice were largely devoid of T cells (Fig. 4b).

Treatment of normal SCID mice with SEB did not result in any intestinal histopathology (Fig. 5). In contrast, when SCID mice which had been reconstituted with a mixed lymphocyte population or purified CD4⁺ T cells were challenged with 5 μ g of SEB and jejunal segments were examined 4 h later, there were obvious changes in gut form (Table 4; Fig. 5) that were reminiscent of those in intestines from SEB-treated immunocompetent BALB/c mice. Thus, 4 h after challenge the villi were swollen, there was increased epithelial vacuolation, there was evidence of tissue hypertrophy, and neutrophils occurred in the submucosa. Villus height was significantly reduced by $\sim 20\%$, and there was an ~ 30 to 35% increase in crypt height, causing an $\sim 40\%$ reduction in the villus: crypt ratio (Table 4). In contrast to BALB/c mice, the increase in crypt depth was still apparent 48 h after SEB challenge of the CD4⁺ T-cell-reconstituted SCID mice. All of the T-cell-reconstituted SCID mice that were challenged with SEB displayed clinical signs of diarrhea, and on autopsy the gut lumens were noticeably fluid filled.

DISCUSSION

SAGs are produced by at least 20 species of bacteria (4) and have been identified as potent stimulants of T-cell activity. While the immunomodulatory properties of SAGs are the focus of extensive research efforts, we have sought to complement such studies by an assessment of the impact of SAGs on gut form and function (20). Here we show that SEB treatment (as a model SAG) causes a self-limiting enteropathy that is char-

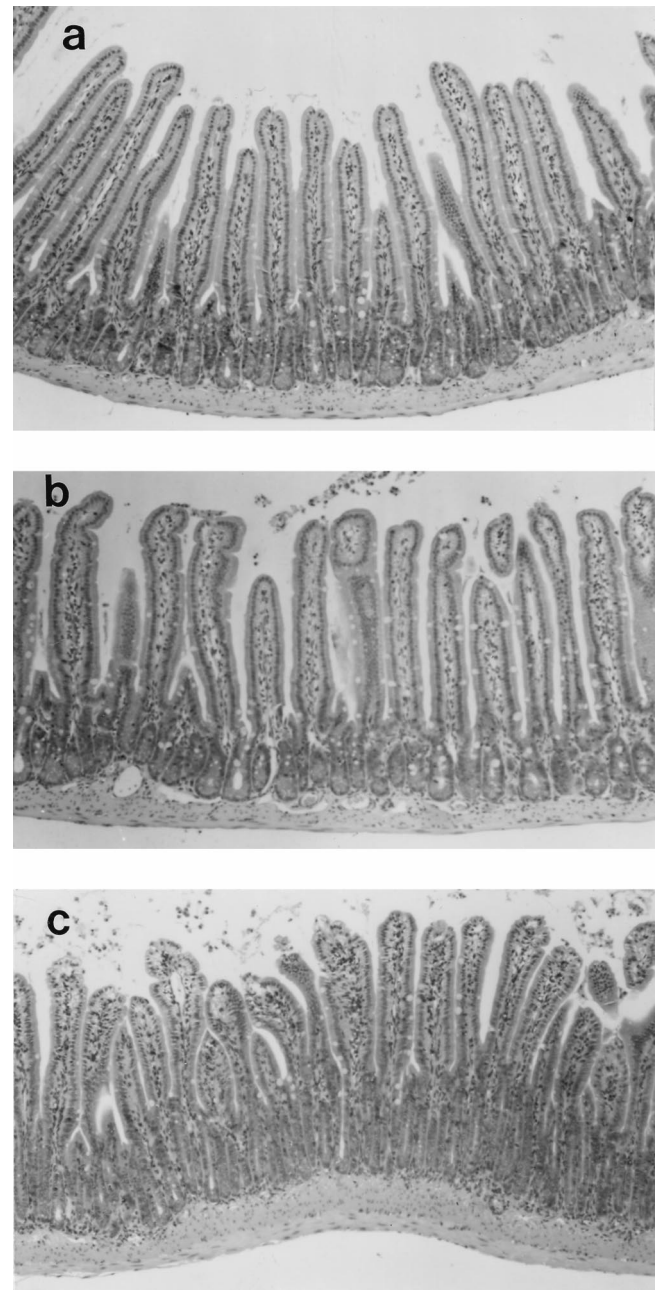


FIG. 5. Photomicrographs of jejunal segments from a control SCID mouse (a) a SCID mouse treated 4 h previously with 5 μ g of SEB (b), and a CD4⁺-reconstituted SCID mouse 4 h after SEB treatment (c). Jejunal segments from control and SEB-treated mice were virtually indistinguishable, whereas T-cell-reconstituted mice responded to SEB with a decrease in villus height and increased crypt depth. Magnification, $\times 100$.

TABLE 4. Jejunal villus-crypt structure in SCID mice with or without SEB treatment^a

Mouse strain or type ^b	Time (h) of SEB treatment	Villus height (μm)	Crypt depth (μm)	Villus: crypt ratio
SCID (control)		330 \pm 20	99 \pm 4	3.2 \pm 0.1
SCID	4	306 \pm 10	110 \pm 3	2.8 \pm 0.1
SCID	12	304 \pm 21	96 \pm 4	3.2 \pm 0.3
SCID	48	319 \pm 6	105 \pm 5	3.0 \pm 0.1
recon-SCID	4	272 \pm 17*	129 \pm 7*	2.1 \pm 0.2*
recon-SCID	48	317 \pm 20	127 \pm 8*	2.6 \pm 0.3*
CD4 ⁺ T-cell-SCID	4	266 \pm 10*	136 \pm 2*	2.0 \pm 0.3*

^a Treated mice received a single i.p. injection of 5 μg of SEB at the indicated times before sacrifice. Values are means \pm SEM; $n = 3$ to 5. *, $P < 0.05$ compared to control.

^b recon-SCID, SCID mice reconstituted with BALB/c spleen and mesenteric lymph node cells; CD4⁺ T-cell-SCID, SCID mice reconstituted with purified CD4⁺ T cells.

acterized by histological changes and altered jejunal villus-crypt architecture.

Having confirmed that SEB evoked an immune response, as evidenced by elevated IL-2 (20, 25) and MHC II expression, the enteric effects of SEB were assessed. Jejunal segments from mice treated with SEB (5 or 100 μg) revealed various degrees of histopathology, typically in the form of slight edema, vacuolation in the epithelial cells, and reduced villus height and increased crypt depth. These changes were apparent 4 h after treatment with SEB and were prolonged following treatment with the high dose of SEB (i.e., 100 μg). Similar findings have been reported by Kent (15) and Merrill and Sprinz (24), who observed swollen villi, elongated crypts, and vacuolated epithelium containing degenerate mitochondria in jejunal tissue from Rhesus monkeys treated 1 to 4 h previously with staphylococcal enterotoxin. The mechanism(s) responsible for the rapid SEB-induced histopathology and derangement of the normal villus-crypt structure is unclear but could be contraction-relaxation of the subepithelial supporting scaffold of myofibroblasts, volume changes in the enterocytes, or alterations in the rate of crypt stem cell proliferation relative to the rate of cell apoptosis and/or necrosis. Clearly, these alterations in villus-crypt morphology could impact on the ability of the epithelium to absorb nutrients and to selectively transport electrolytes (which creates the driving force for directed water movement). Indeed, we have presented data showing that jejunal segments from SEB-treated mice have a reduced capacity to actively transport ions in response to electrical nerve stimulation and the pro-secretory agents carbachol and forskolin (20). Furthermore, employing an in vitro model consisting of monolayers of the human colonic T84 epithelial cell line and peripheral blood mononuclear cells, we showed that SEB-elicited immune activation resulted in increased epithelial permeability and diminished ion transport responses (23).

In addition to villus-crypt changes, SEB-treated (100 μg , 48 h) mice showed increased MHC II expression and an increased number of T cells in the jejunum; many of these cells were in an intraepithelial location or juxtaposed to the epithelial basement membrane. In comparison with this finding, rats treated with *S. aureus* enterotoxin A showed increased numbers of duodenal intraepithelial lymphocytes 30 to 45 min after treatment (3). The physiological significance of these events remains to be determined, but with the indulgence of speculation, at least two possible consequences can be envisaged. First the increase in the number of T cells per villus length would potentiate T-cell paracrine regulation of gut function.

Second, elevated levels of MHC II would permit enhanced immune reactivity. For example, MHC II-positive epithelial cells can present SAGs to T cells, causing increased proliferation and IL-2 receptor expression (1). Thus, the combination of increased numbers of T cells and MHC II expression could lead to a state of enhanced immune responsiveness in the gut that could result in pathophysiological reactions or the exaggeration of subclinical disease or evoke disease relapses (6).

Having identified that SEB evoked significant changes in murine jejunal structure and cellularity, we examined the putative role of T cells, and CD4⁺ T cells in particular, in this enteropathy. T cells have been consistently identified as a critical cell type in the host response to bacterial SAGs (4, 8). For instance, normal mice experience a transient drop (10 to 20%) in body weight in response to SEB, and this does not occur in T-cell-deficient (nude) mice (19). Also, explants of human fetal intestine incubated with SEB displayed a decrease in the surface area-to-volume ratio and an increase in crypt cell proliferation (16). These intestinal changes were accompanied by T-cell activation (increased IL-2 and gamma interferon [IFN- γ]) and were reduced by treatment with the T-cell immunosuppressant FK506. In a modification of this system, the same authors found that T-cell activation by an anti-CD3 monoclonal antibody caused more dramatic changes in fetal enteric morphology ex vivo and a depletion of goblet cells (9). In comparison with this latter observation we noted a slight reduction in PAS-positive goblet cells 48 h after treating mice with the high dose of SEB.

In the present study we found that SEB challenge of SCID mice caused negligible changes in jejunal morphology. However, SCID mice repopulated with mixed lymphocytes or CD4⁺ T cells were responsive to SEB, and the resultant histopathology was as severe as that observed in normal BALB/c mice. In fact, SEB challenge of SCID mice reconstituted with CD4⁺ T cells resulted in an accumulation of fluid in the intestine 4 h after treatment that was more pronounced than that observed in normal SEB-treated BALB/c mice. Collectively, these data illustrate the T-cell dependency of the SEB-induced enteropathy and indicate that CD4⁺ T cells can mediate the enteric response to SAGs. The CD4⁺ T-cell helper cell phenotype can be divided into T helper 1 (T_{h1}) (IL-2- and IFN- γ -producing) and T helper 2 (T_{h2}) (IL-4- and IL-10-producing) subtypes. The relative roles of T_{h1} versus T_{h2} cytokines in SEB-evoked changes in gut function were not examined here. However, previous studies with an in vitro coculture model (see above) have shown that SEB-evoked immune activation causes decreased epithelial irregularities that were prevented by addition of neutralizing antibodies against IFN- γ and tumor necrosis factor α (TNF- α) to the culture well (23). Both of these cytokines can, directly or indirectly, influence epithelial ion transport and permeability (12, 18, 21, 28). In further support of a T_{h1}-type cytokine being involved with SAG-elicited responses, there is a rapid increase in murine serum levels of TNF- α and IFN- γ in response to SEB (25) and human lamina propria lymphocytes and intraepithelial cells produce substantial amounts of TNF- α in response to in vitro SEB challenge (33).

Our data indicate a critical role for CD4⁺ T cells in SEB-induced enteropathy. However, we do not dismiss a role for other cells such as CD8⁺ T cells, mast cells, and MHC II-positive fibroblasts in the intestinal response to SEB; all of these cell types have been found to respond to SEB (11, 26, 31). Having shown that T cells (at least CD4⁺ cells) are critical for the manifestation of the SEB-induced enteropathy, it may be the interaction of various cell types via intricate cell signal-

ling pathways that results in the rapid change in gut morphology following SEB treatment.

In summary, the present study shows that SEB-treated normal, but not T-cell-deficient, mice develop a self-limiting enteropathy that typically involves various degrees of histopathology and an altered villus-crypt ratio. We conclude that exposure to bacterial SAGs can result in rapid changes in gut morphology that are T cell dependent (we have provided data to show direct CD4⁺ T-cell involvement) and suggest that these changes in gut form and cellularity may predispose the host to more rapid or enhanced responses to other antigen(s).

ACKNOWLEDGMENTS

This work was supported by a grant from the Crohn's and Colitis Foundation of Canada to D. M. McKay.

We thank D.P. Snider for the gift of the anti-MHC II antibody used in this study. The technical expertise of B. Hewlett in the immunocytochemical aspects of this work is gratefully acknowledged.

REFERENCES

- Aisenberg, J., E. C. Ebert, and L. Mayer. 1993. T cell activation in human intestinal mucosa: the role of superantigens. *Gastroenterology* **105**:1421-1430.
- Ansell, J. D., and G. J. Bancroft. 1989. The biology of the SCID mutation. *Immunol. Today* **10**:322-325.
- Beery, J. T., S. L. Taylor, L. R. Schlunz, R. C. Freed, and M. S. Bergdoll. 1984. Effects of staphylococcal enterotoxin A on the rat gastrointestinal tract. *Infect. Immun.* **44**:234-240.
- Blackman, M. A., and D. L. Woodland. 1995. *In vivo* effects of superantigens. *Life Sci.* **57**:1717-1735.
- Braegger, C. P., and T. T. MacDonald. 1994. Immune mechanisms in chronic inflammatory bowel disease. *Ann. Allergy* **72**:135-141.
- Brocke, S., A. Gaur, C. Piercy, A. Gautam, K. Gijbels, C. G. Fathman, and L. Steinman. 1993. Induction or relapsing paralysis in experimental autoimmune encephalomyelitis by bacterial superantigen. *Nature* **365**:642-644.
- Conrad, B., E. Weldmann, G. Trucco, W. Rudert, R. Behboo, C. Ricordi, H. Rodriguez-Rilo, D. Finegold, and M. Trucco. 1994. Evidence for superantigen involvement in insulin dependent diabetes mellitus aetiology. *Nature* **371**:351-355.
- Drake, C. G., and B. L. Kotzin. 1992. Superantigens: biology, immunology, and potential role in disease. *J. Clin. Immunol.* **12**:149-162.
- Evans, C. M., A. D. Phillips, J. A. Walker-Smith, and T. T. MacDonald. 1992. Activation of lamina propria T cells induces crypt epithelial proliferation and goblet cell depletion in cultured human fetal colon. *Gut* **33**:230-235.
- Florquin, S., Z. Amraoui, D. Abramowicz, and M. Goldman. 1994. Systemic release and protective role of IL-10 in staphylococcal enterotoxin B induced shock in mice. *J. Immunol.* **153**:2618-2623.
- Herrmann, T., S. Baschieri, R. Lees, and H. R. MacDonald. 1992. *In vivo* responses of CD4⁺ and CD8⁺ cells to bacterial superantigens. *Euro. J. Immunol.* **22**:1935-1938.
- Holmgren, J., J. Fryklund, and H. Larson. 1989. Gamma-interferon-mediated down-regulation of electrolyte secretion by intestinal epithelial cells: a local immune mechanism? *Scand. J. Immunol.* **30**:499-503.
- Ibbotson, J., and J. Lowes. 1995. Potential role of superantigen induced activation of cell mediated immune mechanisms in the pathogenesis of Crohn's disease. *Gut* **36**:1-4.
- Johnson, H. M., J. K. Russel, and C. H. Pontzer. 1991. Staphylococcal enterotoxin superantigens. *Proc. Soc. Exp. Biol. Med.* **198**:765-771.
- Kent, T. H. 1965. Staphylococcal enterotoxin gastroenteritis in rhesus monkeys. *Am. J. Pathol.* **48**:387-407.
- Lionetti, P., J. Spencer, E. J. Breese, S. H. Murch, J. Taylor, and T. T. MacDonald. 1993. Activation of mucosal Vβ8⁺ T cells and tissue damage in human small intestine by the bacterial superantigen, *Staphylococcus aureus* enterotoxin B. *Eur. J. Immunol.* **23**:664-668.
- MacDonald, H. R., S. Baschieri, and R. K. Lees. 1991. Clonal expansion precedes anergy and death of Vβ8⁺ peripheral T cells responding to staphylococcal enterotoxin B *in vivo*. *Eur. J. Immunol.* **21**:1963-1966.
- Madara, J. L., and J. Stafford. 1989. Interferon-γ directly affects barrier function of cultured intestinal epithelial cells. *J. Clin. Invest.* **83**:724-727.
- Marrack, P., M. A. Blackman, E. Kushnir, and J. Kappler. 1990. The toxicity of staphylococcal enterotoxin B in mice is mediated by T cells. *J. Exp. Med.* **171**:455-464.
- McKay, D. M., M. Benjamin, and J. Lu. CD4⁺ T cells mediate superantigen-induced abnormalities in murine jejunal ion transport. *Am. J. Physiol.*, in press.
- McKay, D. M., K. Croitoru, and M. H. Perdue. 1996. T cell monocyte interactions regulate epithelial physiology in a coculture model of inflammation. *Am. J. Physiol.* **270**:C418-C428.
- McKay, D. M., D. W. Halton, C. F. Johnston, I. Fairweather, and C. Shaw. 1990. *Hymenolepis diminuta*: changes in intestinal morphology and the enterochromaffin cell population associated with infection in male C57 mice. *Parasitology* **101**:107-113.
- McKay, D. M., and P. K. Singh. 1997. Superantigen-activation of immune cells evokes epithelial (T84) transport and barrier abnormalities via interferon-γ and tumour necrosis factor-α. Inhibition of increased permeability, but not diminished secretory responses by transforming growth factor β₂. *J. Immunol.* **159**:2382-2390.
- Merrill, T., and H. Sprinz. 1968. The effect of staphylococcal enterotoxin on the fine structure of the monkey jejunum. *Lab. Invest.* **18**:114-123.
- Miethke, T., C. Wahl, K. Heeg, B. Echtenacher, P. H. Krammer, and H. Wagner. 1992. T cell mediated lethal shock triggered in mice by the superantigen staphylococcal enterotoxin B: critical role of tumour necrosis factor. *J. Exp. Med.* **175**:91-98.
- Mourad, W., R. Al-Daccak, T. Chatila, and R. S. Geha. 1993. Staphylococcal superantigens as inducers of signal transduction in MHC class II-positive cells. *Semin. Immunol.* **5**:47-55.
- Paliard, X., S. G. West, J. A. Lafferty, J. R. Clements, J. W. Kappler, P. Marrack, and B. L. Kotzin. 1991. Evidence for the effects of a superantigen in rheumatoid arthritis. *Science* **253**:325-329.
- Perdue, M. H., and D. M. McKay. 1996. Mucosal regulators and immunopathophysiology. *Curr. Opin. Gastroenterol.* **12**:591-599.
- Posnett, D. N., I. Schmelkin, D. A. Burton, A. August, H. McGrath, and L. F. Mayer. 1990. T cell antigen receptor V gene usage: increases in Vβ8⁺ T cells in Crohn's disease. *J. Clin. Invest.* **85**:1770-1776.
- Sartor, R. B. 1995. Current concepts of the etiology and pathogenesis of ulcerative colitis and Crohn's disease. *Gastroenterol. Clin. N. Am.* **24**:475-507.
- Scheuber, P. H., C. Denzlinger, D. Wilker, G. Beck, D. Keppler, and D. K. Hammer. 1987. Staphylococcal enterotoxin B as a nonimmunological mast cell stimulus in primates: the role of endogenous cysteinyl leukotrienes. *Int. Arch. Allergy Appl. Immunol.* **82**:289-291.
- Scott, D., W. Kisch, and A. Steinberg. 1993. Studies of T cell deletion and T cell anergy following *in vivo* administration of SEB to normal and lupus-prone mice. *J. Immunol.* **150**:664-672.
- Sperber, K., L. Silverstein, C. Brusco, C. Yoon, G. E. Mullin, and L. Mayer. 1995. Cytokine secretion induced by superantigens in peripheral blood mononuclear cells, lamina propria lymphocytes, and intraepithelial lymphocytes. *Clin. Diagn. Lab. Immunol.* **2**:473-477.
- Wahl, C., T. Miethke, K. Heeg, and H. Wagner. 1993. Clonal deletion as a direct consequence of an *in vivo* T cell response to bacterial superantigen. *Eur. J. Immunol.* **23**:1197-1200.